APPLIED AND ENVIRONMENTAL MICROBIOLOGY, Nov. 2006, p. 7331–7338 Vol. 72, No. 11
0099-2240/06/$08.00+0 doi:10.1128/AEM.01187-06

Effects of Mutations in the Substrate-Binding Domain of Poly[(*R*)-3-Hydroxybutyrate] (PHB) Depolymerase from *Ralstonia pickettii* T1 on PHB Degradation▽

Tomohiro Hiraishi,[1]* Yoko Hirahara,[2] Yoshiharu Doi,[2] Mizuo Maeda,[1] and Seiichi Taguchi[3]

Bioengineering Laboratory, RIKEN Institute, 2-1 Hirosawa, Wako-shi, Saitama 351-0198, Japan[1]; Polymer Chemistry Laboratory, RIKEN Institute, 2-1 Hirosawa, Wako-shi, Saitama 351-0198, Japan[2]; and Division of Biotechnology and Macromolecular Chemistry, Graduate School of Engineering, Hokkaido University, Sapporo 060-8628, Japan[3]

Received 23 May 2006/Accepted 30 August 2006

Poly[(*R*)-3-hydroxybutyrate] (PHB) depolymerase from *Ralstonia pickettii* T1 ($PhaZ_{RpiT1}$) adsorbs to denatured PHB (dPHB) via its substrate-binding domain (SBD) to enhance dPHB degradation. To evaluate the amino acid residues participating in dPHB adsorption, $PhaZ_{RpiT1}$ was subjected to a high-throughput screening system consisting of PCR-mediated random mutagenesis targeted to the SBD gene and a plate assay to estimate the effects of mutations in the SBD on dPHB degradation by $PhaZ_{RpiT1}$. Genetic analysis of the isolated mutants with lowered activity showed that Ser, Tyr, Val, Ala, and Leu residues in the SBD were replaced by other residues at high frequency. Some of the mutant enzymes, which contained the residues replaced at high frequency, were applied to assays of dPHB degradation and adsorption, revealing that those residues are essential for full activity of both dPHB degradation and adsorption. These results suggested that $PhaZ_{RpiT1}$ adsorbs on the surface of dPHB not only via hydrogen bonds between hydroxyl groups of Ser in the enzyme and carbonyl groups in the PHB polymer but also via hydrophobic interaction between hydrophobic residues in the enzyme and methyl groups in the PHB polymer. The L441H enzyme, which displayed lower dPHB degradation and adsorption abilities, was purified and applied to a dPHB degradation assay to compare it with the wild-type enzyme. The kinetic analysis of the dPHB degradation suggested that lowering the affinity of the SBD towards dPHB causes a decrease in the dPHB degradation rate without the loss of its hydrolytic activity for the polymer chain.

Poly[(*R*)-3-hydroxyalkanoate]s (PHAs) are produced by a wide variety of bacteria and show a remarkable biodegradability in natural environments such as soil (11, 19), activated sludge (33), freshwater (20), and seawater (21). Because of their biodegradability and physical properties, which are comparable to those of conventional plastics, PHAs have attracted academic and industrial interest (1, 5, 9). Poly[(*R*)-3-hydroxybutyrate] (PHB), which is found in many types of bacteria, exists in different states in the cells and after extraction from the cells. In the cells, PHB forms amorphous granules (native PHB [nPHB]) and can be degraded by intracellular PHB depolymerases, which are produced by the PHB-accumulating bacterium itself. After nPHB is extracted from the cells, nPHB is converted to a semicrystalline form (denatured PHB [dPHB]), which can be enzymatically degraded by extracellular PHB depolymerases (dPHB depolymerases) secreted from various microorganisms in the environment.

A number of dPHA depolymerases have been purified and characterized (9, 13), and over 20 dPHA depolymerase genes have been cloned and analyzed (9, 15, 26). Genetic analyses of the enzymes have shown that dPHB depolymerases consist of a catalytic domain at the N terminus, a substrate-binding domain (SBD) at the C terminus, and a linker region connecting the two domains. The structure-function relationship of dPHB depolymerases has been studied extensively, and several mutants were designed to analyze the function of the each domain. Behrends et al. revealed by using a truncated enzyme that the C-terminal domain of dPHB depolymerase (PhaZ4) from *Pseudomonas lemoignei* is essential for dPHB-specific binding (2). Our previous research using SBD-deleted mutants of dPHB depolymerase from *Pseudomonas stutzeri* demonstrated that each domain of dPHB depolymerase functions independently (7). Similarly, Nojiri and Saito genetically prepared many mutants of dPHB depolymerase from *Ralstonia pickettii* T1 (formally known as *Alcaligenes faecalis* T1) ($PhaZ_{RpiT1}$) in various forms, including mutants with substrate-binding domain deletions, inversions, chimeras, and fusions to extralinker domains (24). Their result suggested that the SBD of the enzyme is essential for the degradation of crystalline dPHB material, but not for that of water-soluble substrates, and that the SBD organization of the enzyme influences the degradation of dPHB. Kasuya et al. prepared the fusion proteins of the SBDs of several dPHB depolymerases with glutathione *S*-transferase (12, 14, 25, 29, 30) and investigated the enzymatic adsorption behavior on various polymer surfaces such as PHAs and polysaccharide, indicating that there are some specific interactions based on molecular recognition between SBD and the surfaces of polyesters.

Thus far, there has not been an examination of which amino acid residues in the SBDs of dPHB depolymerases participate in the enzymatic adsorption to the dPHB surface and how these amino acids contribute to the enzymatic adsorption. In this study, we have investigated the interaction between dPHB

* Corresponding author. Mailing address: Bioengineering Laboratory, RIKEN Institute, 2-1 Hirosawa, Wako-shi, Saitama 351-0198, Japan. Phone: 81-48(467)9312. Fax: 81-48(462)4658. E-mail: thiraish@riken.jp.

▽ Published ahead of print on 8 September 2006.

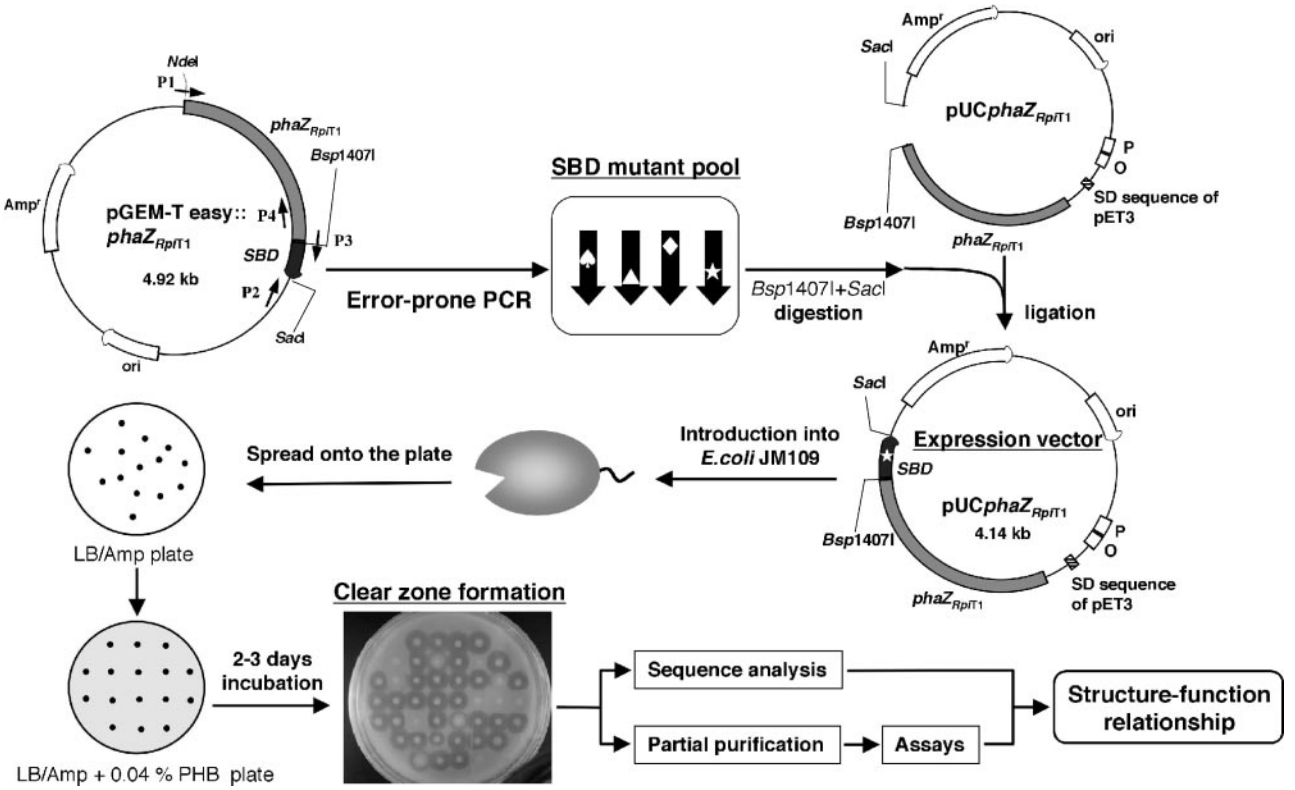

FIG. 1. In vivo assay system for assessment of mutational effects of the substrate-binding domain of $PhaZ_{RpiT1}$ on dPHB degradation. A schematic flow diagram of the system is illustrated. This system is composed of PCR-mediated random mutagenesis in the substrate-binding domain region of $PhaZ_{RpiT1}$ gene, preparation of a mutant library, primary plate assay of dPHB degradation (clear-zone formation), nucleotide sequencing, and assays of dPHB degradation and adsorption by partially purified mutant enzymes.

depolymerase and the dPHB surface by a combination of PCR random mutagenesis targeted only to the SBD region and an in vivo screening system in order to identify the amino acid residues relating to dPHB adsorption. Some of the mutants with amino acid substitutions found in more than three independently isolated clones were partially purified and examined to evaluate the relationship between substrate-binding and dPHB degradation abilities. Furthermore, a kinetic study on the degradation of dPHB granules by the purified enzymes is reported.

MATERIALS AND METHODS

Materials, bacterial strains, and genetic procedures. Purified PHB was purchased from Polyscience, Inc. All of the restriction enzymes and modifying enzymes for genetic engineering were purchased from Takara Bio Inc. and Toyobo. The enzymes were used under conditions recommended by the suppliers. All other chemicals were of biochemical grade and were used without further purification. *Escherichia coli* JM109 was used as a host for transformation with plasmids and for expression of dPHB depolymerase. Preparation of plasmid DNA from *E. coli* and transformation of *E. coli* were carried out according to standard procedures (27).

Construction of an in vivo assay system. An approximately 1,500-bp DNA fragment encoding the signal peptide, catalytic domain, linker region, and SBD was amplified by using genomic DNA from *Ralstonia pickettii* T1 as a template. Two synthetic oligonucleotides, primer 1 (5′-AAGGTGAGGAGACCATATG GTGAGAAGACTG-3′) and primer 2 (5′-GATCGCCCCGAGCTCCCGGCG AGGTCGTCAT-3′), served as primers for PCR amplification. An NdeI restriction site was introduced at the 5′ end of primer 1, and a SacI restriction site was introduced at the 5′ end of primer 2. PCR conditions were as follows: denaturation at 94°C for 30 s, annealing at 68°C for 30 s, and polymerization at 72°C for 2 min with i-Cycler (Bio-Rad). The PCR product was digested with NdeI and SacI and introduced into pUC*phaJ* (34) pretreated with the same restriction enzymes. To introduce a Bsp1407I-restricted site upstream of the SBD, two oligonucleotide primers, primers 3 (5′-AAATCGGCCTTCACCTGTACAGCC ACCACGG-3′) and 4 (5′-CGTCGTCGCCGATACGGCGGCGGAGGGTTG-3′), were designed in inverted tail-to-tail directions to amplify the cloning vector together with the target sequence (Fig. 1). After PCR with these primers, amplified linear DNA was self-ligated, and the resultant plasmid, pUC$phaZ_{RpiT1}$, transformed JM109 competent cells. pUC$phaZ_{RpiT1}$ carries a native signal sequence of $PhaZ_{RpiT1}$ for potential periplasmic localization to form the disulfide bridges which are essential for its activity.

Figure 1 shows a scheme for PCR-mediated mutagenesis and the screening system for dPHB depolymerase ($PhaZ_{RpiT1}$) mutants. A pGEM-T Easy vector containing the PCR product of $phaZ_{RpiT1}$ was used as a template for PCR mutagenesis with primers 2 and 3. The target region, including only the SBD, was amplified with the two primers under error-prone PCR conditions as described previously (32) with slight modifications. After amplification, the product was restricted with Bsp1407I and SacI and ligated into pUC$phaZ_{RpiT1}$ pretreated with the same restriction enzymes. The resultant plasmid was introduced into *E. coli* JM109, and then the recombinant *E. coli* was spread on Luria-Bertani (LB) medium plates containing 100 μg/ml of ampicillin. When the recombinant *E. coli* was cultivated on LB medium plates containing dPHB granules (0.04% PHB granules, 0.5 mM isopropyl-β-D-thiogalactopyranoside [IPTG], and 100 μg/ml of ampicillin) at 30°C overnight to form colonies, detectable clear zones due to degradation of the dPHB granules appeared around the colonies after an additional 1 day of incubation at 30°C. Changes in degradation activity of the mutant dPHB depolymerases were judged on the basis of the formation of the clear zone. Secretion of the enzymes from the recombinants was examined by immunoprecipitation with anti-$PhaZ_{RpiT1}$ on LB agar plates (containing 0.5 mM IPTG and 100 μg/ml of ampicillin).

Assays of partially purified mutant enzymes. Partial purification of $PhaZ_{RpiT1}$ mutant enzymes was carried out as follows. The recombinant *E. coli* mutants were cultivated in 1.75 ml of LB medium with 100 μg/ml of ampicillin at 30°C. After 3 to 3.5 h, 0.5 mM IPTG (final concentration) was added to the culture

medium, and then the cells were harvested by centrifugation after an additional 4 h of cultivation. The collected cells were resuspended in 200 μl of 10 mM phosphate buffer (pH 7.0), sonicated, and centrifuged. The resultant soluble fraction was applied to a HiTrap Q HP column (Amersham Biosciences). The enzyme protein was eluted in the nonadsorbed fraction and stored at −80°C.

A dPHB adsorption assay of the partially purified $PhaZ_{RpiT1}$ mutant enzymes was carried out as follows. The enzyme solution (25 μl) was added to 75 μl of 50 mM Tris-HCl buffer (pH 7.5) containing 0.4 g/liter of dPHB granules and incubated at 30°C for 10 min. The reaction mixture was centrifuged at 21,500 × *g* for 2 min to obtain the soluble fraction. A control experiment was also carried out in the absence of the granule to estimate the total enzyme. By Western dot blot analysis, the relative amount of the enzyme bound to dPHB granule was calculated from the equation $[E]_{ad} = ([E]_{tot} - [E]_{sol})/[E]_{tot} \times 100$ (%), where $[E]_{ad}$, $[E]_{sol}$, and $[E]_{tot}$ are the concentrations of adsorbed enzyme, nonadsorbed enzyme, and total enzyme, respectively. The enzymatic solutions were dropped on a nitrocellulose membrane, and the $PhaZ_{RpiT1}$ enzymes were detected by using an antiserum raised against $PhaZ_{RpiT1}$. An anti-rabbit immunoglobulin G conjugated with alkaline phosphatase was then applied, and the enzymes were stained with nitroblue tetrazolium and 5-bromo-4-chloro-3-indolylphosphate. Dot intensities were analyzed on a Macintosh (OS 9.2) computer using the public domain NIH Image program (developed at the U.S. National Institutes of Health and available on the Internet at http://rsb.info.nih.gov/nih-image/). dPHB granule degradation by the mutant enzymes was performed in 50 mM of Tris-HCl buffer (pH 7.5) containing 0.4 g/liter dPHB granule and 1.0 mM $CaCl_2$. The reaction was started by the addition of 20 μl of enzymatic solution to 200 μl of the reaction mixture at 30°C and was monitored at 595 nm by using a Bio-Rad model 550 microplate reader with a 595-nm filter. Esterase activity was determined spectrophotometrically with *para*-nitrophenylbutyrate (PNPB) as a water-soluble substrate. The reaction was started by the addition of enzymatic solution to 300 μl of the reaction mixture containing 0.5 mM PNPB in 10 mM phosphate buffer (pH 7.0) at 30°C and measured at 405 nm. One unit of enzyme was defined as the amount of protein required to increase the value of absorbance at 405 nm by 1 per min.

Enzyme purification. Recombinant *E. coli* harboring the wild-type or L441H mutant enzyme gene was cultivated at 28°C to an optical density (OD) at 600 nm of 0.6, after which 0.5 mM IPTG (final concentration) was added to the culture medium. After addition of IPTG, recombinant *E. coli* was cultivated at 25°C overnight. The cells were harvested by centrifugation at 3,500 × *g* and 4°C for 10 min. The collected cells were suspended in 10 mM phosphate buffer (pH 7.0), and disrupted with a French press three times at 14,000 lb/in^2. Crude cell extracts were centrifuged at 15,000 × *g* and 4°C for 20 min and filtered with 0.2-μm cellulose acetate filter.

All purification procedures were carried out at 0 to 4°C. The resultant supernatant was applied to Toyopearl butyl-650S column (25 ml; Tosoh) preequilibrated with 10 mM phosphate buffer (pH 7.0) containing 3.0 M ammonium sulfate. The enzyme was eluted with a linear gradient of 3.0 to 0 M ammonium sulfate for three bed volumes followed by a linear gradient from 0 to 40% ethanol for three bed volumes. The enzyme fractions were collected, dialyzed against 10 mM potassium phosphate buffer (pH 7.0), and applied to a Q Sepharose FF column (25 ml; Amersham Biosciences). The enzymatic activity was found in nonadsorbed fractions. The eluted enzyme fractions were collected, concentrated, and stored at −80°C.

Assay of dPHB degradation by purified enzymes. The dPHB-degrading activities of the purified enzymes were assayed as follows. A reaction mixture containing 0.4 g of dPHB granule and 1.0 mM $CaCl_2$ was prepared in 1.0 liter of 50 mM Tris-HCl buffer (pH 7.5). The reaction was started by the addition of enzyme to 2.0 ml of the reaction mixture at 37°C and was monitored at 600 nm (Shimadzu MultiSpec-1500 spectrophotometer equipped with temperature controller). To evaluate the effect of enzyme concentration on dPHB degradation, the reaction rates were measured by setting the enzyme concentrations in the range of 0.25 to 3.5 μg/ml. Curve fitting was performed by using Grafit curve-fitting software (Erithacus Software).

Analytical procedures. Sodium dodecyl sulfate-polyacrylamide gel electrophoresis (SDS-PAGE) was performed according to the procedure of Laemmli (18) with a molecular weight calibration kit (Bio-Rad). Protein was stained with Coomassie brilliant blue R250 (Kanto Chemical). Protein concentrations were determined by the method of Bradford (3) with the protein assay kit II (Bio-Rad), and bovine serum albumin was used as a standard. The nucleotide sequence was determined with a Beckman Coulter CEQ2000XL sequencer and the *Taq* dye terminator cycle sequencing kit (Beckman Coulter). The DNA and deduced amino acid sequences were analyzed by using the sequence analysis program GENETYX (Software Development Co.).

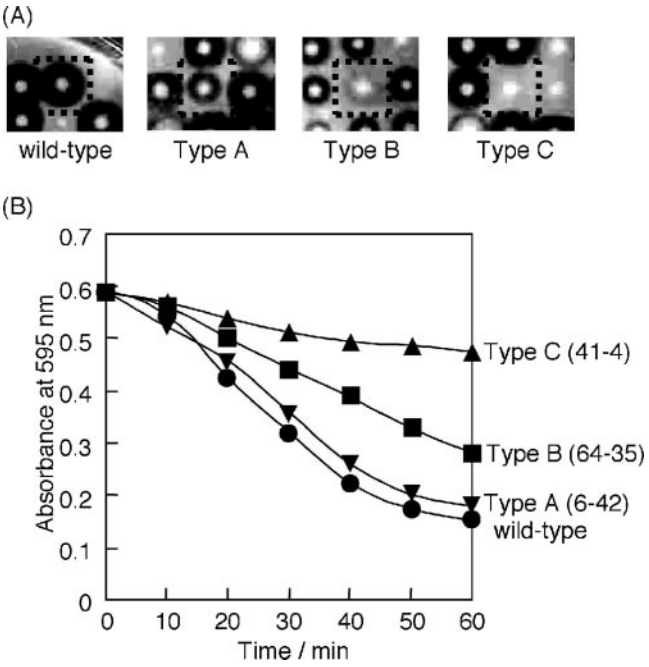

FIG. 2. (A) Phenotypes of mutants obtained by PCR-mediated mutagenesis on in vivo dPHB degradation assay. Type A, mutants forming clear but smaller halos; type B, mutants forming normal-size but opaque halos; type C, mutants forming no halos. (B) Time dependence of changes in turbidity during dPHB granule degradation by partially purified mutant and wild-type $PhaZ_{RpiT1}$. The partially purified mutant enzymes were added to a 0.4-g/liter dPHB granule suspension at 30°C and monitored at 595 nm.

RESULTS

Construction of an in vivo system for mutational analysis of $PhaZ_{RpiT1}$. In order to screen the mutated $PhaZ_{RpiT1}$ with altered dPHB-degrading ability, an in vivo assay system for mutational analysis of $PhaZ_{RpiT1}$ was developed by combining PCR random mutagenesis with a clear-zone formation assay to measure the dPHB degradation level of recombinant *E. coli* JM109 (Fig. 1). Recombinant *E. coli* JM109 carrying the wild-type $PhaZ_{RpiT1}$ gene secreted $PhaZ_{RpiT1}$ from its periplasmic space and formed a clear zone around colonies after 2 days cultivation at 30°C (Fig. 2A). This system was designed so that the level of dPHB degradation was attributed only to the change in dPHB-binding ability of $PhaZ_{RpiT1}$ by maintaining the level of $PhaZ_{RpiT1}$ activity for a water-soluble substrate, because the error-prone PCR was performed only in the gene region localized for the SBD. A mutant library of $PhaZ_{RpiT1}$ genes was prepared by colony formation by transformant cells of *E. coli* JM109. Based on clear-zone formation around the colonies grown on the dPHB plate, non-dPHB-degrading clones, probably caused by the loss of dPHB-binding ability or extracellular production of $PhaZ_{RpiT1}$, were estimated to be approximately 15% of a total of 4,000 clones.

Relationship between clear-zone formation pattern and dPHB-degrading ability of the mutants. All of the clones thus obtained were classified into three types of mutants based on the pattern of clear-zone formation compared with that of the recombinant *E. coli* strain producing the wild-type enzyme, where the wild-type enzyme produced a distinct clear halo

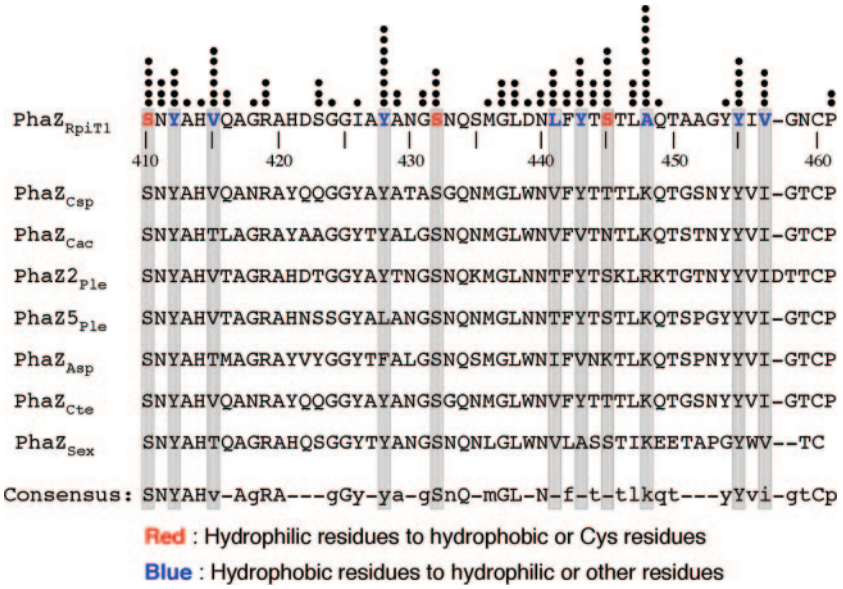

FIG. 3. Positions and frequencies of PCR-mediated single mutations in the region coding for the SBD of $PhaZ_{RpiT1}$, together with alignment of SBDs of other dPHB depolymerases. The sequences of the dPHB depolymerases from *R. pickettii* T1 ($PhaZ_{RpiT1}$), *Comamonas acidovorans* ($PhaZ_{Cac}$), *P. lemoignei* ($PhaZ2_{Ple}$ and $PhaZ5_{Ple}$), *Acidovorax* sp. strain TP_4 ($PhaZ_{Asp}$), *Comamonas testosteroni* ($PhaZ_{Cte}$), and *Streptomyces exfoliatus* ($PhaZ_{Sex}$) are shown. Amino acid residues conserved among dPHB depolymerases are indicated by uppercase letters in the consensus sequence; those which are conserved in six or more proteins are indicated by lowercase letters in the consensus sequence. The amino acids that were replaced with other residues at high frequencies in $PhaZ_{RpiT1}$ mutants are shaded. Tendencies of the amino acid substitutions at positions where the amino acids are replaced with high frequencies in $PhaZ_{RpiT1}$ mutants are indicated as colored letters.

around the colony: type A, mutants forming clear but smaller halos; type B, mutants forming opaque but normal-size halos; and type C, mutants forming no halos (Fig. 2A). In this mutant library, several mutants with different clear-zone formation patterns (called phenotypes) were examined to evaluate the correlation between phenotype and dPHB-degrading ability of the mutants. The mutant enzymes, which are probably translocated to the periplasmic space by their signal sequences, were partially purified from the soluble fraction of recombinant *E. coli* cells broken by sonication and eluted from a HiTrap Q column. SDS-PAGE analysis of the eluted enzyme fractions showed that the expression levels of the enzymes were almost indistinguishable among the wild-type and mutant enzymes (data not shown). Figure 2B shows typical profiles of in vitro enzymatic dPHB degradation by the partially purified mutant and wild-type enzymes. The rate of in vitro dPHB degradation by the mutant enzyme 6-42 showed a type A phenotype, comparable to that by the wild-type enzyme, while in vitro dPHB degradation by the 64-35 (type B phenotype) and 41-4 (type C phenotype) mutant enzymes showed reduced rates but these mutants still had almost normal levels of esterase activity for PNPB as a water-soluble substrate (12.5 to 23.0 U/mg) compared to the wild-type enzyme (17.3 U/mg). Thus, the in vitro dPHB degradation rates by the mutants of each phenotype were categorized in the order wild type = type A > type B > type C. As shown in Fig. 2A, the order of the degree of clear zone formation was type A > type B > type C, while the secretion levels of the mutant enzymes from recombinant *E. coli* were comparable to that of the wild type (data not shown). Based on these findings, the amino acid residues in SBD responsible for dPHB binding can be assessed by analyzing mutants screened on the basis of the plate assay.

Amino acid substitutions in the SBD of $PhaZ_{RpiT1}$. The 150 clones arbitrarily selected from this mutant library were subjected to DNA sequence analysis for identification of the positions where amino acid residues were replaced. Nucleotide sequence analysis of these mutants revealed that the mutants carried one to three point mutations and that the mutations were distributed over the SBD region of $PhaZ_{RpiT1}$. There were 103 single mutants, 31 double mutants, 7 triple mutants, and 9 deletion mutants, which were generated by the insertion of a stop codon, in these clones. Figure 3 shows the amino acid substitutions in the 103 single mutants. The single mutations were distributed over the SBD coding region, but not randomly. Figure 3 also shows the alignment of amino acid sequences of SBDs of other dPHB depolymerases, and the amino acid residues corresponding to the residues replaced at high frequency in $PhaZ_{RpiT1}$ mutants are indicated. Most of the highly substituted residues in $PhaZ_{RpiT1}$ (Ser410, Ser432, Tyr412, Tyr428, Tyr443, Tyr455, and Val415) are conserved among other dPHB depolymerases, while Leu441, Ser445, and Val457 were not highly conserved but were replaced by other residues with similar hydropathy properties observed in other dPHB depolymerases. In addition, the Ala448 residue was replaced at the highest frequency in $PhaZ_{RpiT1}$ mutants, but this residue is replaced by positively charged residues such as Lys and Arg in other dPHB depolymerases. The amino acid positions where amino acid substitutions were found in more than three independently isolated clones are listed in Table 1. Most of these single amino acid substitutions resulted in phenotypes of normal-size opaque halos (type B) formed by *E. coli* mutants.

Assays of adsorption and degradation by partially purified mutant enzymes. The partially purified wild-type enzyme and

TABLE 1. Positions, genotypes, and phenotypes of mutations in the substrate-binding domain of dPHB depolymerase from *Ralstonia pickettii* T1

Clone	Substitution		Phenotype[a]
	Nucleotide	Amino acid	
Wild type	None		
34-21	AGC→GGC	S410G	B
37-6	AGC→GGC	S410G	B
65-21	AGC→GGC	S410G	B
69-10	AGC→GGC	S410G	B
33-37	AGC→ATC	S410I	B
44-30	TAC→AAC	Y412N	B
6-22	TAC→AAC	Y412N	B
8-20	TAC→AAC	Y412N	B
24-24	TAC→CAC	Y412H	B
19-22	GTG→GCG	V415A	B
35-29	GTG→GCG	V415A	B
79-30	GTG→GCG	V415A	B
32-43	GTG→GAG	V415E	C
65-17	GTG→GAG	V415E	B
35-25	GTG→ATG	V415M	C
10-25	TAC→TGC	Y428C	B
1-25	TAC→TGC	Y428C	B
26-17	TAC→TGC	Y428C	B
29-3	TAC→TGC	Y428C	B
32-5	TAC→TGC	Y428C	B
35-30	TAC→TGC	Y428C	B
6-4	TAC→TGC	Y428C	B
85-32	TAC→TGC	Y428C	B
8-3	TCG→GCG	S432A	B
41-3	TCG→GCG	S432A	B
79-18	TCG→GCG	S432A	B
7-13	TCG→ACG	S432T	A
64-35	CTC→CAC	L441H	B
58-36	CTC→TTC	L441F	B
80-24	CTC→TTC	L441F	B
8-23	CTC→CCC	L441P	B
66-9	TAC→AAC	Y443N	B
29-19	TAC→TGC	Y443C	B
2-33	TAC→CAC	Y443H	B
32-25	TAC→CAC	Y443H	B
67-16	TAC→CAC	Y443H	B
37-16	AGC→TGC	S445C	B
42-37	AGC→TGC	S445C	B
74-37	AGC→TGC	S445C	B
36-10	AGC→GGC	S445G	B
69-3	AGC→GGC	S445G	B
89-41	AGC→GGC	S445G	B
8-1	GCG→GAG	A448E	B
87-43	GCG→GAG	A448E	B
9-17	GCG→GAG	A448E	A/B
83-29	GCG→GGG	A448G	B
10-18	GCG→ACG	A448T	B
49-42	GCG→ACG	A448T	B
32-25	GCG→ACG	A448T	B
76-24	GCG→ACG	A448T	B
81-13	GCG→ACG	A448T	B
81-41	GCG→ACG	A448T	B
86-5	GCG→GTG	A448V	B
79-17	TAC→AAC	Y455N	B
81-18	TAC→AAC	Y455N	B
14-6	TAC→TGC	Y455C	B
31-7	TAC→TGC	Y455C	B
8-2	TAC→TGC	Y455C	B
34-34	GTC→GCC	V457A	B
38-33	GTC→GAC	V457D	B
60-33	GTC→GAC	V457D	C
23-40	GTC→GGC	V457G	B

[a] Type A, mutants forming clear but smaller halos; B, mutants forming opaque but normal-size halos; C, mutants forming no halos.

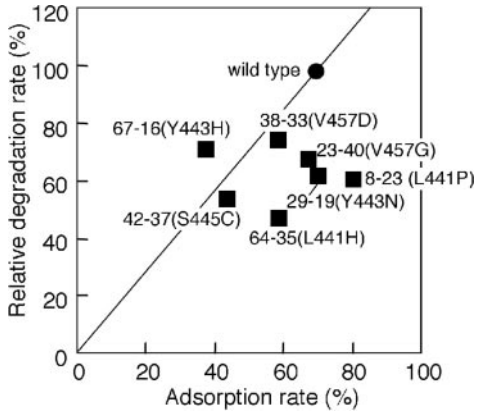

FIG. 4. Relationship between dPHB adsorption and degradation abilities of the mutant $PhaZ_{RpiT1}$. The adsorption assay was performed at 30°C. The rate of in vitro dPHB degradation by the wild-type enzyme was defined as 100%. The clone names and amino acid substitutions are indicated.

some of the mutant enzymes, which were highly substituted at positions of the conserved residues, were subjected to the adsorption assay on dPHB granules as described in Materials and Methods. When the wild-type enzyme was mixed with the dPHB granule solution, 68% ± 8.4% of the total enzyme adsorbed on the dPHB granule. However, when the mutant enzymes were subjected to dPHB adsorption assay, the adsorption rates of the mutants (except L441P, which showed 80% adsorption) were generally lower than that of the wild-type enzyme. The rates for the mutant enzymes were generally distributed over the range of 35 to 70% adsorption.

For the evaluation of the correlation between dPHB adsorption and degradation abilities of the mutant enzymes, in vitro degradation by some of the enzymes having amino acids replaced at positions of the highly conserved residues was carried out. The rates of degradation by the mutant enzymes were plotted against their adsorption rates, as shown in Fig. 4. For Fig. 4, relative in vitro degradation rates were calculated by assuming that the activity of the wild-type enzyme was 100%, while those of the mutant enzymes were distributed over the range of 45 to 80%. In all the mutants except L441P, both the adsorption and relative degradation rates of the mutant enzymes were lower than those of the wild type.

Purification and characterization of the L441H mutant enzyme. It is thought that the mutant enzymes with the lower dPHB degradation abilities contain an amino acid substitution at one of the residues important for dPHB degradation and adsorption. Therefore, to examine the effects of the amino acid substitutions in the SBD region on dPHB degradation, we purified the L441H mutant enzyme with the lowest degradation activity among the partially purified enzymes for further characterization and comparison with the wild-type enzyme. The L441H mutant and wild-type enzymes were purified from the soluble fraction of recombinant *E. coli* JM109 by using a Toyopeal butyl column followed by a Q Sepharose FF column. SDS-PAGE analysis revealed that the collected active fractions were electrophoretically homogeneous for both enzymes (data not shown). The L441H enzyme showed the same binding

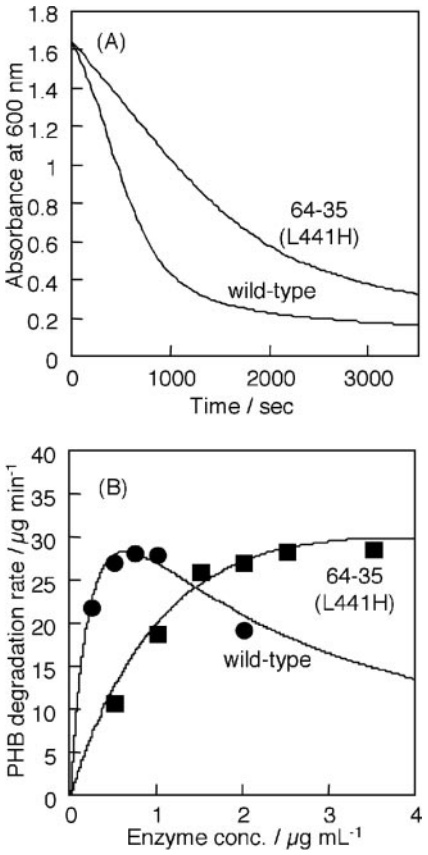

FIG. 5. (A) Time dependence of changes of turbidity during dPHB granule degradation at 37°C by 0.5 μg/ml of the purified L441H mutant and wild-type $PhaZ_{RpiT1}$. (B) Concentration effects of $PhaZ_{RpiT1}$ on the rate of dPHB granule degradation by L441H mutant (■) and wild-type (●) enzymes. The enzymatic dPHB degradation was carried out with wild-type or L441H mutant enzyme concentrations of 0.25 to 3.5 μg/ml. The curves through the points represent the fit to each set of data of the equation $R = k_s K[E]/(1 + K[E])^2$.

properties during the protein purification procedure as the corresponding wild-type enzyme.

Figure 5A shows time-dependent changes in turbidity during the degradation of dPHB granules by 0.5 μg/ml of wild-type and L441H mutant enzymes at 37°C. Upon addition of the wild-type enzyme, the turbidity rapidly decreased with an increase in the reaction time, and the maximum degradation rate was determined as 0.092 OD unit/min. However, when the L441H mutant enzyme was assayed, dPHB degradation by the mutant enzyme proceeded at a maximum rate of 0.037 OD unit/min, about threefold slower the rate for the wild-type enzyme.

Enzyme concentrations of 0.25 to 3.5 μg/ml were used to evaluate the enzyme concentration dependence of dPHB degradation by L441H mutant and wild-type enzymes. Figure 5B shows the effect of dPHB depolymerase concentration on the dPHB granule degradation. On the basis of the linear correlation between optical density and dPHB granule concentration (one OD unit is 150 μg/ml) (28), the degradation rate values were converted from optical density into mass units (μg/min). When the wild-type enzyme was used as the catalyst, the degradation rates increased with enzyme concentrations to reach a maximum value at 0.75 μg/ml. At higher enzyme concentrations, the degradation rates decreased. This phenomenon could be explained in terms of a change of coverage of the film surface by the adsorbed enzyme (22, 37). On the other hand, the dependence of dPHB degradation by the L441H mutant enzyme on the enzyme concentrations differed from that for the wild-type enzyme. The rates of degradation by the L441H mutant enzyme increased with increasing enzyme concentrations, reaching a constant value at an enzyme concentration of 2.5 to 3.5 μg/ml. The maximum rate of degradation by the L441H mutant enzyme was determined to be 29.2 μg/min, comparable to that of the wild-type enzyme (28.6 μg/min). Assuming that the adsorption of the enzyme to the polymer surface obeys a Langmuir isotherm, the degradation behavior was successfully described by a heterogenous kinetic model, which is composed of enzyme adsorption and subsequent hydrolysis of polymer chains (22). The equation can be written as $R = k_s K[E]/(1 + K[E])^2$, where R is the dPHB granule degradation rate, k_s is the surface hydrolysis rate constant, and K is the adsorption equilibrium constant of the enzyme. The kinetic parameters for the wild-type enzyme were calculated as $k_s = 113 \pm 2.3$ μg/min and $K = 1.6 \pm 0.11$ ml/μg, while the k_s and K values for the L441H mutant enzyme were determined as 120 ± 4.2 μg/min and 0.27 ± 0.03 ml/μg, respectively. The k_s value for the L441H mutant enzyme was comparable to that for the wild-type enzyme, while the adsorption constant for the L441H mutant enzyme was apparently lower than that for the wild-type enzyme.

DISCUSSION

In this study, the interactions between dPHB depolymerase amino acid residues and the dPHB surface have been investigated at the molecular level. First, we established a system by combining PCR random mutagenesis targeted only to the SBD region with a clear-zone formation assay for determining dPHB degradation levels of recombinant *E. coli* JM109 on dPHB-containing plates to find residues important for the adsorption and degradation of dPHB. The clear-zone formation patterns (phenotypes) of the recombinants corresponded with the rates of in vitro dPHB degradation by mutant enzymes, which had almost normal levels of esterase activity, purified from each recombinant phenotype, while the secretion levels of the mutant enzymes in the present system were comparable to that of the wild type. These findings indicated that the difference of the phenotypes among the mutants is caused by the inactivation of dPHB binding of the enzymes. Similarly, Jendrossek et al. studied the function of denatured poly(3-hydroxyoctanoate)(dPHO) depolymerase from *Pseudomonas fluorescens* GK13 by PCR random mutagenesis (10). Their results revealed that the phenotypes of the recombinants depended on the dPHO-degrading ability of their mutant enzymes, in which Leu and Phe residues were replaced and probably were involved in the interaction between the enzyme and dPHO.

Gene analysis of 150 clones selected from the mutant library revealed that there were 103 single-amino-acid substitutions, which were distributed over the SBD region of $PhaZ_{RpiT1}$. Amino acid positions where the amino acid substitutions were found in more than three independently isolated clones are listed in Table 1. Ser410, Ser432, Ser445, Tyr412, Tyr428, Tyr443, Tyr455, Val415, Val457, and Ala448 in $PhaZ_{RpiT1}$ were highly

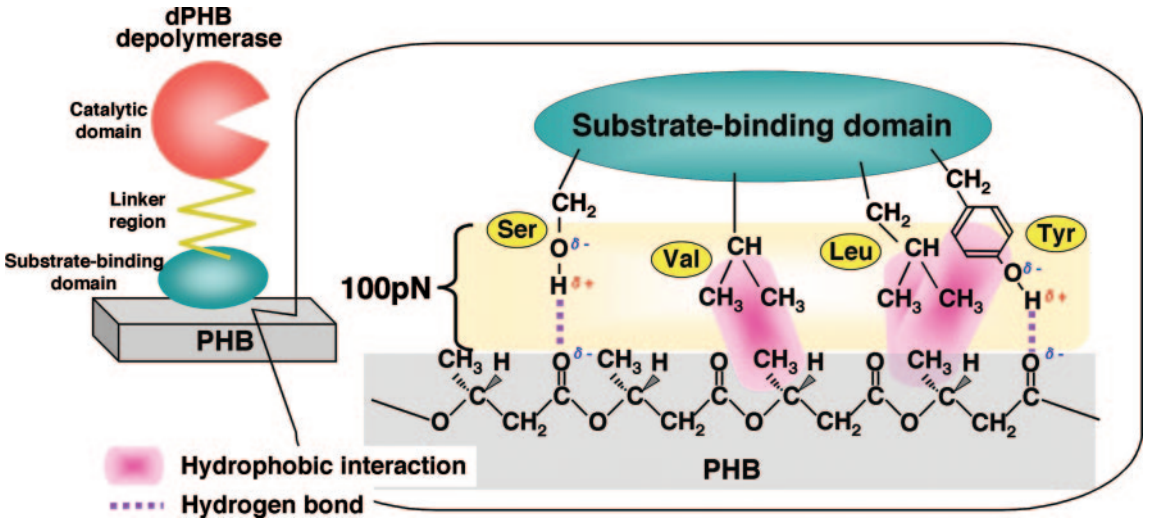

FIG. 6. Schematic illustration of the interaction between the amino acid residues in the SBD of $PhaZ_{RpiT1}$ and the PHB polymer chain.

substituted by other residues in the mutants showing the type B phenotype (mutants forming opaque but normal-size halos), suggesting that these substitutions inhibit the ability of $PhaZ_{RpiT1}$ to bind to dPHB. The tendencies in the amino acid substitutions of these single mutants can be classified into two groups. The first group consisted of replacements of the hydrophilic Ser residue with a hydroxyl group, and the second group included replacements of hydrophobic residues such as Val, Leu, Tyr, and Ala.

Except for S432T, Ser410, Ser432, and Ser445 in the first group (Fig. 3) were replaced by small hydrophobic amino acid residues such as Gly and Ala or by Cys with a thiol group incapable of forming a hydrogen bond. In the case of S432T (type A phenotype), a Ser residue can functionally substitute for Thr with a hydroxyl group, resulting in the normal level of dPHB degradation capacity compared to the wild type (Fig. 2 and Table 1). These findings suggested that these replacements by Gly, Ala, and Cys probably diminish the hydrogen bond strength between the protein and the polymer.

On the other hand, Val415, Val457, Leu441, Ala448, and Tyr455 (Fig. 3) are hydrophobic residues and tended to be replaced as follows. The Ala448 residue tended to be replaced by hydrophilic, acidic residues. At the position of Ala448 in $PhaZ_{RpiT1}$, the positively charged residues such as Lys and Arg are conserved among other dPHB depolymerases, as shown in Fig. 3, suggesting that the Ala residue can functionally substitute for Lys and Arg but the acidic, hydrophilic residues are unable to replace them. The Val415 and Val457 residues had a tendency to be replaced by hydrophilic or small hydrophobic residues, so these substitutions may weaken the hydrophobic interaction between the SBD and the polymer. In the case of Leu441, the replacement by His probably reduces the hydrophobic interaction between them. In addition to the replacement by His, this residue was replaced by Phe or Pro, which have hydrophobic but bulky characteristics, suggesting that steric hindrance by the bulky residues may occur upon adsorption of the mutants to dPHB. Tyr 412, Tyr428, Tyr443, and Tyr455, which are bulky and nonpolar except for the hydroxyl group, were replaced by Cys, Asn, or His residues, which have hydrophilic characteristics, suggesting the decrease of the hydrophobic interaction. Even if the Tyr residues participate in the hydrophilic interactions via their hydroxyl group, these substitutions may weaken them since the hydrogen bond distance between the amine and carbonyl groups (NH—O, 0.30 nm) is longer than that between hydroxyl and carbonyl groups (OH—O, 0.27 nm) (31).

Previous quartz crystal microbalance and atomic force microscopy (AFM) studies with various polymers or surfactants have also suggested that $PhaZ_{RpiT1}$ adsorbs to the dPHB surface via both hydrogen bonds and hydrophobic interactions (6, 36, 37). Hisano et al. determined the crystal structure of single-domain dPHB depolymerase from *Penicillium funiculosum* (8). They proposed that hydrophobic residues, including Tyr, Leu, Ile, and Val, contribute to adsorption to the dPHB surface and that hydrophilic residues (Ser and Asn) located around the mouth of the enzyme crevice may also contribute to the affinity of the enzyme for dPHB. Based on the present findings, the previous results, and the chemical structure of PHB, which contains carbonyl and methyl groups as functional groups, we propose a plausible model of the interaction between the SBD of $PhaZ_{RpiT1}$ and the dPHB surface (Fig. 6). It is implied that the SBD of $PhaZ_{RpiT1}$ has an interactive force with the dPHB polymer surface of about 100 pN (6). This interaction is composed of not only hydrogen bonds between the hydrophilic residues in the enzyme and the ester bonds in the polymer but also of hydrophobic interactions between the hydrophobic residues in the enzyme and the methyl groups in the polymer.

The correlation between adsorption and degradation rates of the enzymes showed that the most of their ratios, especially for L441H and L441P, were lower than that of the wild type (Fig. 4). This finding suggested that the adsorbed L441P and L441H enzymes on the dPHB surface have a lower ability to degrade dPHB than the wild-type enzyme and that the L441 residue probably participates both in the adsorption to the dPHB surface and in the enhancement of dPHB degradation. Our previous AFM studies have revealed that the dPHB depolymerase strongly adsorbed onto the polyester surface, displacing some polyester chains at the adsorption interface and forming

small ridges around the enzyme molecules. This indicates that a strong chemical interaction exists between the SBD of dPHB depolymerase and the polymer chains (16, 17). Furthermore, AFM analysis with PHB single crystals and a mutant of dPHB depolymerase with disrupted hydrolytic activity has demonstrated that the SBD of dPHB depolymerase disturbs the molecular packing of PHB polymer chains, resulting in the fragmentation of PHB single crystals (23). Similarly, in the field of enzymatic degradation of cellulose by cellulase or of chitin by chitinase, several researchers reported that the binding domains of these enzymes enhance the specific physical disruption of their substrates (4, 35). In the present study, the kinetics of the dPHB degradation by wild-type and L441H mutant enzymes was determined in order to assess the mutational effects of substrate-binding ability of the enzyme on the reaction. The kinetic analysis for the L441H mutant enzyme has revealed that this mutant enzyme has less substrate-binding activity than the wild-type enzyme despite retaining the hydrolytic activity for the polymer chain. Taking the present results into consideration, the enzymatic adsorption process of the dPHB depolymerase on the dPHB surface probably consists of both an adsorption reaction of the enzyme to the surface and the nonhydrolytic disruption of the substrate to promote dPHB degradation via several amino acid residues, such as L441.

ACKNOWLEDGMENTS

We especially thank Y. Kikkawa for helpful discussions and C. T. Nomura (SUNY-ESF) for critical reading of our manuscript. We are particularly grateful to T. Hisano for suggestions regarding the interaction between the depolymerase and the polyester surface.

This research was supported by grants for Ecomolecular Science Research from the RIKEN Institute.

REFERENCES

1. **Anderson, A. J., and E. A. Dawes.** 1990. Occurrence, metabolism, metabolic role, and industrial uses of bacterial polyhydroxyalkanoates. Microbiol. Rev. **54:**450–477.
2. **Behrends, A., B. Klingbeil, and D. Jendrossek.** 1996. Poly(3-hydroxybutyrate) depolymerases bind to their substrate by a C-terminal located substrate binding site. FEMS Microbiol. Lett. **143:**191–194.
3. **Bradford, M. M.** 1976. A rapid and sensitive method for the quantitation of microgram quantities of protein utilizing the principle of protein-dye binding. Anal. Biochem. **72:**248–254.
4. **Carrard, G., A. Koivula, H. S. Söderlund, and P. Béguin.** 2000. Cellulose-binding domains promote hydrolysis different sites on crystalline cellulose. Proc. Natl. Acad. Sci. USA **97:**10342–10347.
5. **Doi, Y.** 1990. Microbial polyesters, p. 33–62. VCH Publishers, New York, N.Y.
6. **Fujita, M., Y. Kobori, Y. Aoki, N. Matsumoto, H. Abe, Y. Doi, and T. Hiraishi.** 2005. Interaction between PHB depolymerase and biodegradable polyesters by atomic force microscopy. Langmuir **21:**11829–11835.
7. **Hiraishi, T., T. Ohura, S. Ito, K. Kasuya, and Y. Doi.** 2000. Function of the catalytic domain of poly(3-hydroxybutyrate) depolymerase from *Pseudomonas stutzeri*. Biomacromolecules **1:**320–324.
8. **Hisano, T., K. Kasuya, Y. Tezuka, N. Ishii, T. Kobayashi, M. Shiraki, E. Oroudjev, H. Hansma, T. Iwata, Y. Doi, T. Saito, and K. Miki.** 2006. The crystal structure of polyhydroxybutyrate depolymerase from *Penicillium funiculosum* provides insights into the recognition and degradation of biopolyesters. J. Mol. Biol. **356:**993–1004.
9. **Jendrossek, D.** 2002. Extracellular polyhydroxyalkanoate depolymerases: the key enzymes of PHA degradation., p 41–83 *In* Y. Doi and A. Steinbüchel (ed.), Biopolymers 3b. Wiley-VCH Verlag GmbH, Weinheim, Germany.
10. **Jendrossek, D., A. Schirmer, and R. Handrick.** 1997. Recent advances in characterization of bacterial PHA depolymerases, p. 89–101 *In* G. Eggink, A. Steinbüchel, Y. Poirier, and B. Witholt, (ed.), 1996 International Symposium on Bacterial Polyhydroxyalkanoates. NRC Research Press, Ottawa, Canada.
11. **Kasuya, K., Y. Doi, and T. Yao.** 1994. Enzymatic degradation of poly[(*R*)-3-hydroxybutyrate] by *Comamonas testosteroni* ATSU of soil bacterium. Polym. Degrad. Stab. **45:**379–386.
12. **Kasuya, K., Y. Inoue, T. Tanaka, T. Akehata, T. Iwata, T. Fukui, and Y. Doi.** 1997. Biochemical and molecular characterization of the polyhydroxybutyrate depolymerase of *Comamonas acidovorans* YM1609, isolated from fresh water. Appl. Environ. Microbiol. **63:**4844–4852.
13. **Kasuya, K., H. Mitomo, M. Nakahara, A. Akiba, T. Kudo, and Y. Doi.** 2000. Identification of a marine benthic P(3HB)-degrading bacterium isolate and characterization of its P(3HB) depolymerase. Biomacromolecules **1:**194–201.
14. **Kasuya, K., T. Ohura, K. Masuda, and Y. Doi.** 1999. Substrate and binding specificities of bacterial polyhydroxybutyrate depolymerases. Int. J. Biol. Macromol. **24:**329–336.
15. **Kasuya, K., T. Tanaka, Y. Tezuka, W. C. Hsieh, H. Mitomo, and Y. Doi.** 2003. Cloning, expression and characterization of a poly(3-hydroxybutyrate) depolymerase from *Marinobacter* sp. NK-1. Int. J. Biol. Macromol. **33:**221–226.
16. **Kikkawa, Y., M. Fujita, T. Hiraishi, M. Yoshimoto, and Y. Doi.** 2004. Direct observation of poly(3-hydroxybutyrate) depolymerase adsorbed on polyester thin film by atomic force microscopy. Biomacromolecules **5:**1642–1646.
17. **Kikkawa, Y., K. Yamashita, T. Hiraishi, M. Kanesato, and Y. Doi.** 2005. Dynamic adsorption behavior of poly(3-hydroxybutyrate) depolymerase on polyester surface investigated by QCM and AFM. Biomacromolecules **6:**2084–2090.
18. **Laemmli, U. K.** 1970. Cleavage of structural proteins during the assembly of head of bacteriophage T4. Nature **227:**680–685.
19. **Mergaert, J., A. Webb, C. Anderson, A. Wouters, and J. Swings.** 1993. Microbial-degradation of poly(3-hydroxybutyrate) and poly(3-hydroxybutyrate-*co*-3-hydroxyvalerate) in soils. Appl. Environ. Microbiol. **59:**3233–3238.
20. **Mukai, K., K. Yamada, and Y. Doi.** 1994. Efficient hydrolysis of polyhydroxyalkanoates by *Pseudomonas stutzeri* YM1414 isolated from lake water. Polym. Degrad. Stab. **43:**319–327.
21. **Mukai, K., K. Yamada, and Y. Doi.** 1993. Enzymatic degradation of poly(hydroxyalkanoates) by a marine bacterium. Polym. Degrad. Stab. **41:**85–91.
22. **Mukai, K., K. Yamada, and Y. Doi.** 1993. Kinetics and mechanism of heterogeneous hydrolysis of poly[(R)-3-hydroxybutyrate] film by PHA depolymerases. Int. J. Biol. Macromol. **15:**361–366.
23. **Murase, T., Y. Suzuki, Y. Doi, and T. Iwata.** 2002. Nonhydrolytic fragmentation of a poly[(*R*)-3-hydroxybutyrate] single crystal revealed by use of a mutant of polyhydroxybutyrate depolymerase. Biomacromolecules **3:**312–317.
24. **Nojiri, M., and T. Saito.** 1997. Structure and function of poly(3-hydroxybutyrate) depolymerase from *Alcaligenes faecalis* T1. J. Bacteriol. **179:**6965–6970.
25. **Ohura, T., K. Kasuya, and Y. Doi.** 1999. Cloning and characterization of the polyhydroxybutyrate depolymerase gene of *Pseudomonas stutzeri* and analysis of the function of substrate-binding domains. Appl. Environ. Microbiol. **65:**189–197.
26. **Saito, T., K. Suzuki, J. Yamamoto, T. Fukui, K. Miwa, K. Tomita, S. Nakanishi, S. Odani, J. Suzuki, and K. Ishikawa.** 1989. Cloning, nucleotide sequence, and expression in *Escherichia coli* of the gene for poly(3-hydroxybutyrate) depolymerase from *Alcaligenes faecalis*. J. Bacteriol. **171:**184–189.
27. **Sambrook, J., E. F. Fritsch, and T. Maniatis.** 1989. Molecular cloning: a laboratory manual, 2nd ed. Cold Spring Harbor Laboratory Press, Cold Spring Harbor, N.Y.
28. **Scandola, M., M. L. Focarete, and G. Frisoni.** 1998. Simple kinetic model for the heterogeneous enzymatic hydrolysis of natural poly(3-hydroxybutyrate). Macromolecules **31:**3846–3851.
29. **Shinomiya, M., T. Iwata, and Y. Doi.** 1998. The adsorption of substrate binding domain of PHB depolymerases to the surface of poly(3-hydroxybutyric acid). Int. J. Biol. Macromol. **22:**129–135.
30. **Shinomiya, M., T. Iwata, K. Kasuya, and Y. Doi.** 1997. Cloning of the gene for poly(3-hydroxybutyric acid) depolymerase of *Comamonas testosterone* and functional analysis of its substrate-binding domain. FEMS Microbiol. Lett. **154:**89–94.
31. **Stryer, L.** 1988. Biochemistry, 3rd ed. W. H. Freeman and Company, New York, N.Y.
32. **Taguchi, S., A. Maehara, K. Takase, M. Nakahara, and Y. Doi.** 2001. Analysis of mutational effects of a polyhydroxybutyrate (PHB) depolymerase on bacterial PHB accumulation using an in vivo assay system. FEMS Microbiol. Lett. **198:**65–71.
33. **Tanio, T., T. Fukui, Y. Shirakura, T. Saito, K. Tomita, T. Kaiho, and S. Masamune.** 1982. An extracellular poly(3-hydroxybutyrate) depolymerase from *Alcaligenes faecalis*. Eur. J. Biochem. **124:**71–77.
34. **Tsuge, T., T. Hisano, S. Taguchi, and Y. Doi.** 2003. Alteration of chain length substrate specificity of *Aeromonas caviae R*-enantiomer-specific enoyl-coenzyme A hydratase through site-directed mutagenesis. Appl. Environ. Microbiol. **69:**4830–4836.
35. **Vaaje-Kolstad, G., S. J. Horn, D. M. F. van Aalten, B. Synstad, and V. G. H. Eijsink.** 2005. The non-catalytic chitin-binding protein CBP21 from *Serratia marcescens* is essential for chitin degradation. J. Biol. Chem. **280:**28492–28497.
36. **Yamashita, K., Y. Aoyagi, H. Abe, and Y. Doi.** 2001. Analysis of adsorption function of polyhydroxybutyrate depolymerase from *Alcaligenes faecalis* T1 by using a quartz crystal microbalance. Biomacromolecules **2:**25–28.
37. **Yamashita, K., T. Funato, Y. Suzuki, S. Teramachi, and Y. Doi.** 2003. Characteristic interactions between poly(hydroxybutyrate) depolymerase and poly[(*R*)-3-hydroxybutyrate] films studied by a quartz crystal microbalance. Macromol. Biosci. **3:**694–702.